Ultrarapid catalytic reduction of some dyes by reusable novel erythromycin-derived silver nanoparticles

Yasmeen JUNEJO[1,2], **Abdulhadi BAYKAL**[1,*]

[1]Department of Chemistry, Fatih University, Büyükçekmece, İstanbul, Turkey

[2]National Center of Excellence in Analytical Chemistry, University of Sindh Jamshoro, Jamshoro, Pakistan

Abstract: A novel green approach for the synthesis of silver nanoparticles using erythromycin as a reducing/capping agent is presented. Erythromycin-derived silver nanoparticles were characterized by ultraviolet-visible spectroscopy, scanning electron microscopy, high resolution transmission electron microscopy, X-ray powder diffraction, and Fourier transform infrared spectroscopy. Monodispersed silver nanoparticles showed excellent and promising catalytic activity for reduction of 3 differently charged dyes (eosin B, methylene blue, and rose bengal) in the presence of $NaBH_4$. The study revealed that 100% reduction of these dyes can be achieved efficiently in just 150–250 s. They were easily recovered from the reaction medium and were reused 5 times, showing enhanced catalytic potential each time. Glass-supported Ag(0) NPs (0.15 mg) were removed by washing sequentially and reused 5 times for catalytic reduction of these dyes at 10 μM. All dyes were successfully reduced by erythromycin-derived silver nanoparticles up to 7%. Based upon these results, it was concluded that erythromycin-derived silver nanoparticles are a novel, rapid, and highly economical alternative for environmental protection against pollution caused by dyes and can be extended for the control of other reducible contaminants.

Key words: Inorganic compounds, chemical synthesis, X-ray diffraction, catalytic properties

1. Introduction

Metallic silver is an increasingly important material in several technologies either in bulk form or finely discrete. Silver displays exclusive properties associated with the noble metals (excellent electrical conductivity, chemical stability, catalytic activity), besides other more precise ones (antibacteriostatic effects, nonlinear optical behavior, etc.).[1] Silver nanoparticles (Ag(0) NPs) have attracted attention due to their surface plasmon resonance, which can be easily monitored by UV-visible spectrophotometer.[2] Previously silver nanoparticles were prepared by several methods like hydrothermal synthesis,[3] sonochemical method,[4] and electron beam irradiation[5] using many other reducing agents like 3,4-ethylenedioxythiophene (EDOT),[6] ibuprofen (analgesic),[7] and cefditoren (antibiotic).[8] Some researchers used plant extract for the synthesis of silver nanoparticles.[9−11] Silver possesses several characteristics like significant size- and shape-dependent optical properties, major efficiency of surface plasmon excitation, and the highest electrical and thermal conductivity in bulk among all metals.[3] These distinctive properties have led to promising applications of silver nanoparticles in the fields of catalysis,[8,12] development of nanosensors,[7] antimicrobial activity,[13−17] and so on.

---

*Correspondence: hbaykal@fatih.edu.tr

Today, dyes are among the most common organic industrial pollutants. Dyes liberated as waste products from the textile, plastics, paper, food, leather, and cosmetic industries etc. are a major source of toxic species in the form of colored wastewater. These colored species are posing a great threat in the photosynthetic process in aquatic plants due to meager light penetration.[18−21] Moreover, some azo dyes and their degradation products such as aromatic amines are highly carcinogenic.[22] Many processes have been implemented for decolorization of dyes using methods such as adsorption,[23] degradation,[24−26] oxidation,[27,28] and catalytic reduction.[29−32] However, in order to save energy and having safer operations together with avoiding use of organic solvents, it would be interesting and meaningful to develop a new process for detoxification in aqueous solution under mild conditions with minimal energy consumption. Furthermore, this new process could be used for treatment of wastewater containing mainly dyes without complicated composition.

The aim of this study was to synthesize small Ag(0) NPs and to further investigate their activity as a heterogeneous, recoverable, and reusable catalyst for exceptionally faster and complete reduction of the dyes eosin B (EB), rose bengal (RB), and methylene blue (MB). To the best of our knowledge, there is no simple and quick method by which erythromycin-derived Ag(0) NPs are reported for catalysis of dyes at room temperature. Herein we report a novel, easy, rapid, and one-step method for synthesis of well-stabilized Ag(0) NPs and their catalytic activity.

2. Results and discussion

2.1. UV-Vis study

UV-Vis spectroscopy was used to optimize various parameters such as concentration of different ingredients like silver nitrate, erythromycin standard, and sodium hydroxide. Very small and blue-shifted nanoparticles were synthesized using 0.5% solution of $AgNO_3$, 0.5% standard, and 0.01 M NaOH. The UV-Vis spectra were recorded after 1 h (Figure 1a) of preparation of the solution when a light yellow color appeared, which indicates the synthesis of Ag(0) NPs.[8] The UV-Vis spectra showed an absorbance peak of Ag(0) NPs at 420 nm as shown in Figures 1a and 1b. It was also confirmed from the literature[17,33] that Ag(0) NPs show absorbance between 380 and 450 nm. Figure 1 shows a small increase in the absorbance of the prepared Ag(0) NPs up to 24 h (Figure 1b). Graphical representation of the synthesis of Ag(0) NPs is presented in the Scheme.

2.2. FT-IR study

The capping of Ag(0) NPs by erythromycin can be explained with the help of observations made in IR studies. It is evident that the region between 3500 and 3200 cm^{-1} represents OH stretching peaks.[34] The vibration peak at 3467 cm^{-1} for erythromycin was shifted towards 3461 cm^{-1} in Ag(0) NPs and the intensity of the peak was also affected at the same time. In plane bending of OH at 1378 cm^{-1}[7] for erythromycin, the standard shifted to 1384 cm^{-1} for the Ag(0) NPs and it reveals the presence of this group being attached and bonded with Ag(0) NPs. The peak at 1637 cm^{-1} shows asymmetric –COO, which is present in the standard and also in nanoparticles (Figure 2a and 2b). The peaks at 1457 and 1373 cm^{-1} are present in the standard but these peaks shift towards 1381 cm^{-1} in Ag(0) NPs; it further indicates the bonding of the CO bond. It shows that the CO group of erythromycin standard undergoes bonding with silver in the formation of silver nanoparticles. Therefore, it is clearly indicated from the FT-IR study that silver can be attached with 2 functional groups, OH and CO (Figure 2b).
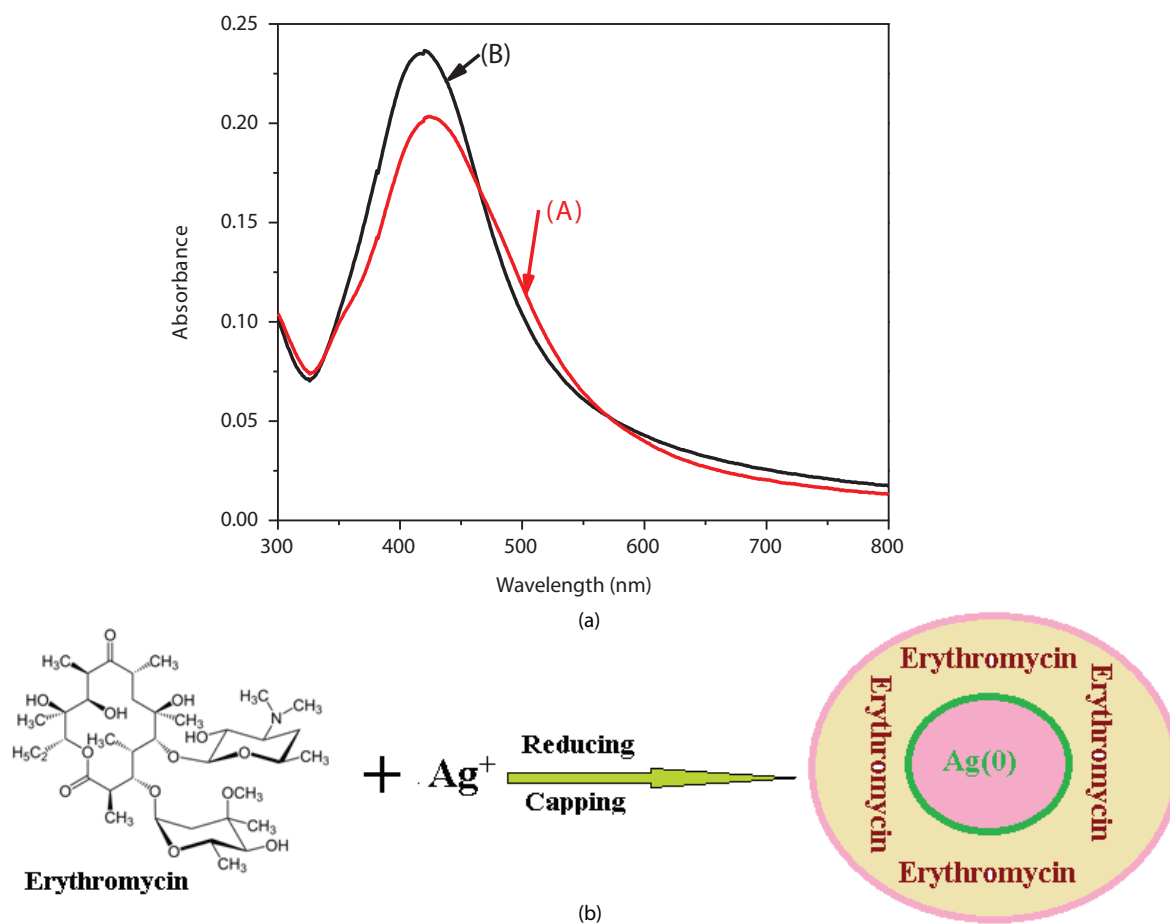
Figure 1. a) UV-Vis spectra showing the formation of silver nanoparticles after 1 h (A) and after 24 h (B). b) Graphical representation of synthesis of Ag(0) NPs.
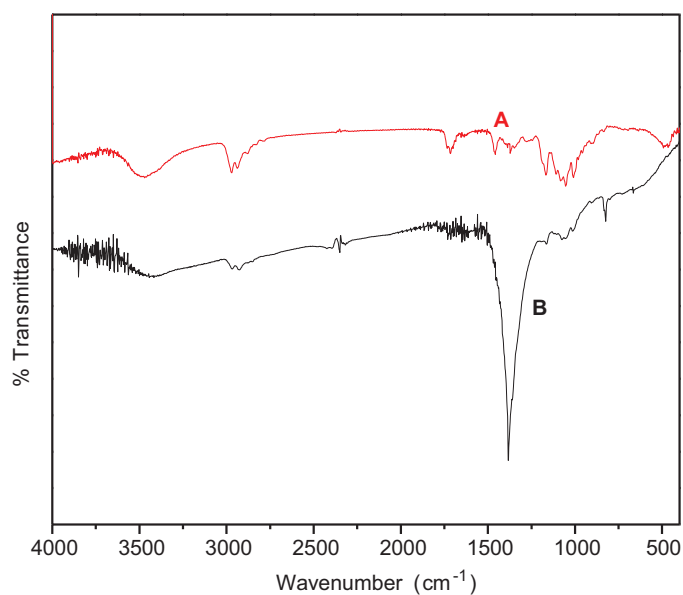

Figure 2. FT-IR spectra of erythromycin standard (A) and erythromycin-reduced silver nanoparticles (B).

2.3. SEM study

SEM images of Ag(0) NPs are indicated after 10 min of mixing of all the solutions (Figure 3). According to the previous image, it was observed that most of the particles were cylindrical rod-like in the range of 11 × 33 nm–76 × 597 nm with an average size of 56 × 288 nm. There were also some very fine nanospheres, nanorods, or nanowires with very small dimensions. Even some scattered nanorods ranging from 11 × 28 nm to 62 × 288 nm are also seen in Figure 3.
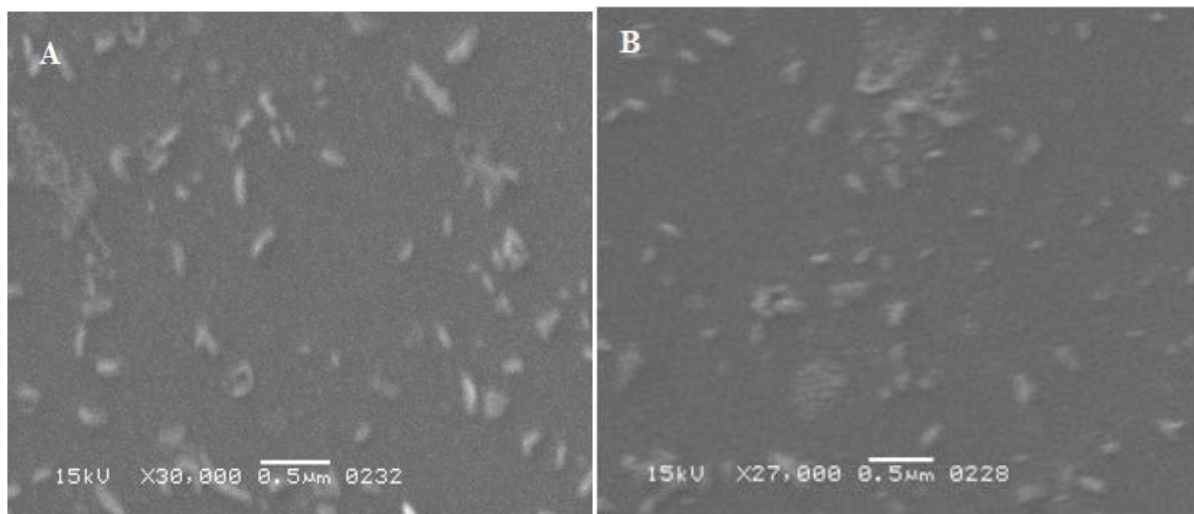

Figure 3. SEM micrographs of Ag(0) NPs formed by the reduction of AgNO$_3$ with erythromycin.

2.4. HR-TEM analysis

The morphology of Ag(0) NPs was investigated by HR-TEM. It was observed that small and monodispersed Ag(0) NPs were synthesized with the help of antibiotic. The particle size of Ag(0) NPs was calculated as 14.2 ± 3.1 nm and they were spherical as shown in Figure 4. A number of methods have been reported for synthesis of Ag(0) NPs and characterized by HR-TEM.[8] These smaller monodispersed nanospheres promise to have superior catalytic activity for some specific applications.
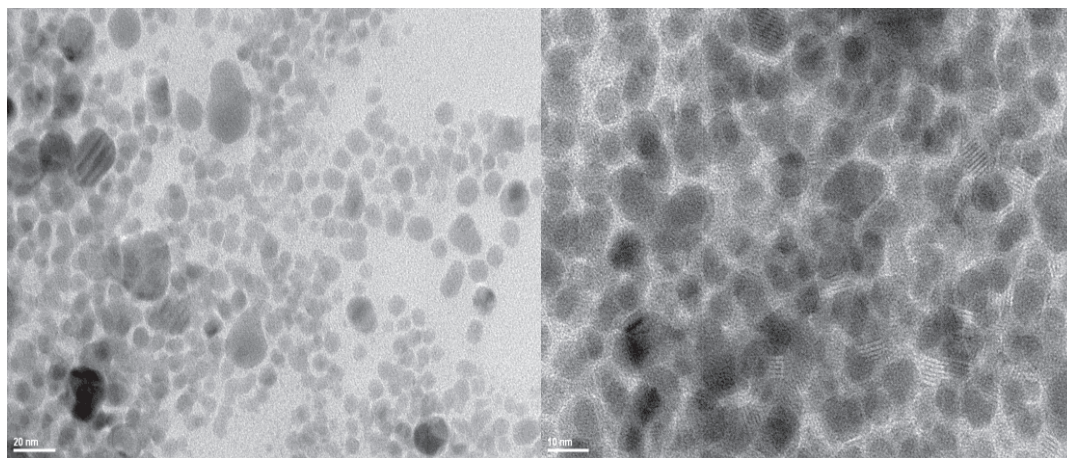

Figure 4. HR-TEM images of Ag(0) NPs formed by the reduction of AgNO3 with erythromycin.

2.5. XRD study

XRD powder pattern with line profile fitting of Ag(0) NPs is presented in Figure 5. Nearly 2 mg of dark black solid sample was analyzed having Ag(0) NPs with a face centered cubic (FCC) structure.[35,36] The mean size of the crystallites was estimated from the powder diffraction pattern by implementing line profile fitting using Eq. (1) as given in Wejrzanowski et al.[37] The calculated crystallite size was found to be 13 ± 4 nm.
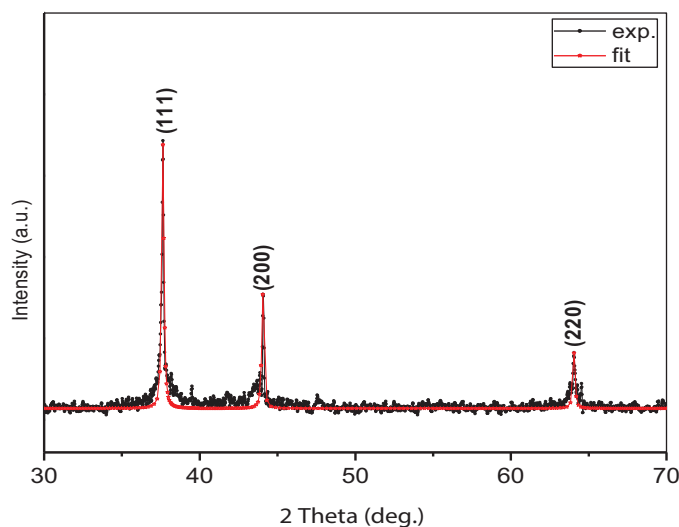

Figure 5. XRD powder pattern of Ag(0) NPs with line profile fitting.

2.6. Reduction of MB

To examine the catalytic efficiency of Ag(0) NPs in an aqueous system, MB was selected. MB showed surface plasmon resonance at 662 nm. Actually MB is cationic in nature. As indicated in Figure 6a, there is no reduction of MB in the absence of $NaBH_4$. A very small reduction of MB was observed with $NaBH_4$ in the absence of Ag(0) NPs for 1 h. It was observed that in the absence of catalyst the strong reducing agent $NaBH_4$ was unable to reduce MB. It reduced MB up to 7.7%. Reduction of MB was done by $NaBH_4$; Figure 6a shows the reduction of 10 μL of MB without $NaBH_4$ and Figure 6b shows the reduction of 10 μL of MB with 200 μL of 0.1 M $NaBH_4$ (spectra were taken 1 h after the addition of $NaBH_4$).

We then compared our results with previously published results.[2] It was noted that the reduction of dyes by $NaBH_4$ did not occur to an appreciable extent in the absence of Ag(0) NPs. However, the catalytic efficiency of Ag(0) NPs can be confirmed from Figure 6b. This indicates the reduction of dye in the presence of Ag(0) NPs. For the catalysis study, Ag(0) NPs were pasted over a glass cover slip. With the addition of glass-supported Ag(0) NPs, the reduction of dye took place within 200 s. This reaction was observed by the help of a UV-Vis spectrophotometer. The surface plasmon resonance peak was seen to gradually decrease with the addition of glass-supported Ag(0) NPs and then resulted in final disappearance, as shown in Figure 6b.

2.7. Reduction of RB

The catalytic activity of small Ag(0) NPs was checked for the reduction of RB by applying $NaBH_4$ as reducing agent. The mixture of RB and $NaBH_4$ was examined for 24 h and a very small reduction was noted (Figure 7a). RB reduction was done in the presence of $NaBH_4$; 10 μL of RB without $NaBH_4$ (Figure 7a) and 10 μL of

RB + 200 μL of 0.1 M NaBH$_4$ (Figure 7a). The small Ag(0) NPs exhibited an excellent catalytic response and complete reduction took place within 250 s. RB showed a characteristic peak at 547 nm; this band decreased very sharply with the addition of Ag(0) NPs in 200 s (Figure 7b).
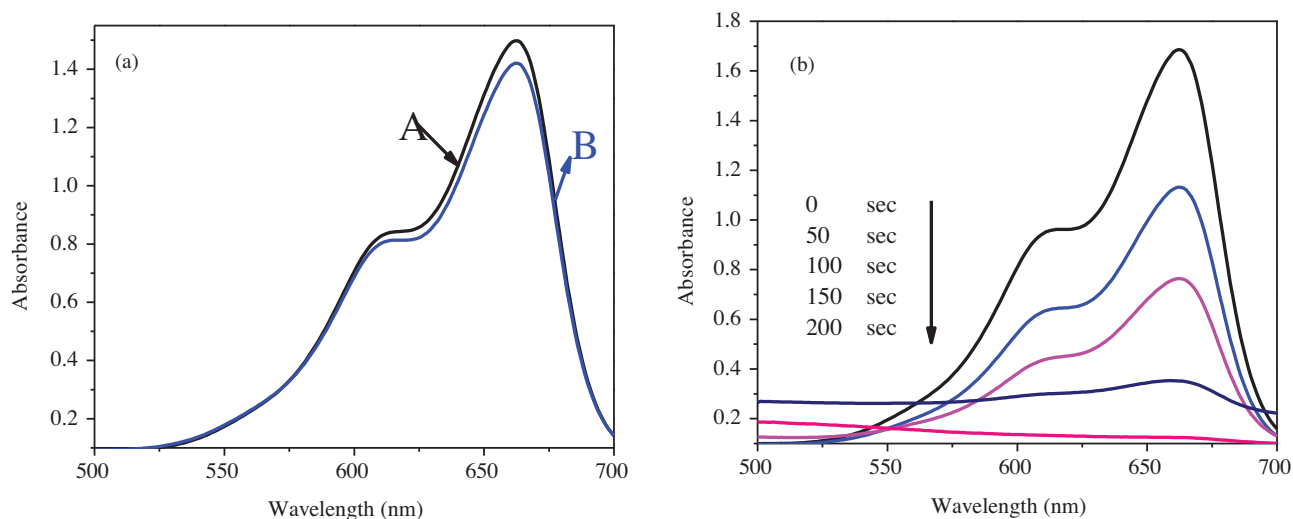

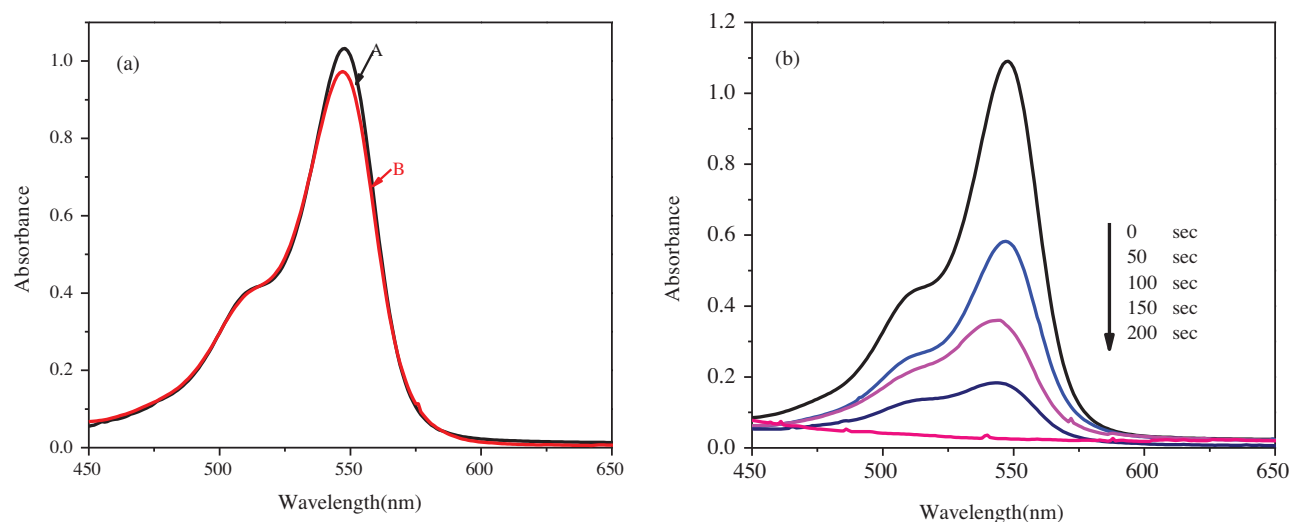**Figure 6.** Reduction of MB dyes in the presence of (a) NaBH$_4$ and (b) with catalyst Ag(0) NPs.

Figure 7. Reduction of RB dyes in the presence of (a) NaBH$_4$ and (b) with catalyst Ag(0) NPs.

2.8. Reduction of EB

To explore the efficiency of Ag(0) NPs in an aqueous system, EB showed surface plasmon resonance at 515 nm. A small reduction of EB was observed with NaBH$_4$ in the absence of Ag(0) NPs for 1 h. It was observed that in the absence of catalyst the strong reducing agent NaBH$_4$ was unable to reduce EB. It reduced EB up to 8.7% (Figure 8a). The reduction of eosin B was done in the presence of NaBH$_4$, 10 μL of EB without NaBH$_4$ (Figure 8a), and 10 μL of EB + 200 μL of 0.1 M NaBH$_4$ (Figure 8a). Reduction of dye by NaBH$_4$ did not occur to an appreciable extent in the absence of Ag(0) NPs; however, the catalytic efficiency of Ag(0)

NPs can be confirmed from Figure 8b. This indicated the reduction of dye in the presence of Ag(0) NPs. Dye showed a complete reduction reaction in 250 s and the product of this reaction was completely colorless after the reduction.
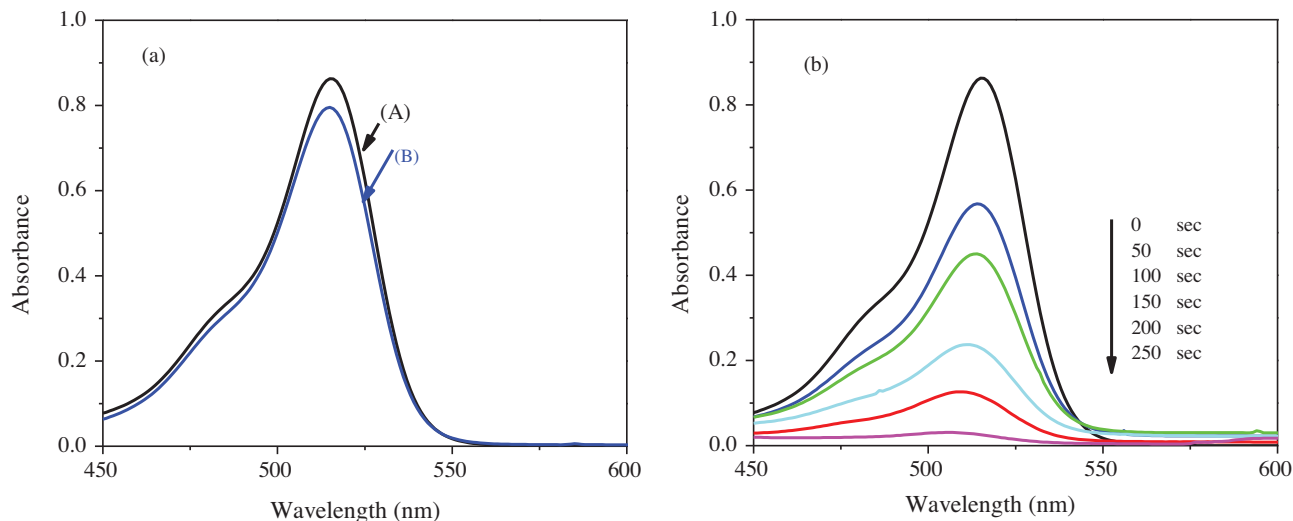

Figure 8. Reduction of EB dyes in the presence of (a) $NaBH_4$ and (b) with catalyst Ag(0) NPs.

2.9. Recycling and reuse of Ag(0) NPs

Glass-supported Ag(0) NPs (0.15 mg) were removed by washing sequentially and reused 5 times for catalytic reduction of these dyes at 10 μM. The reducing potential of recovered and reused Ag(0) NPs for MB, RB, and EB was calculated (Figures 9a–9c). The potential of Ag(0) NPs for bleaching of color was apparent. However, the decrease in the activity of Ag(0) NPs was still not very low. This behavior confirmed that recovered Ag(0) NPs were highly active even with some possible loss during each repeated washing. The slow deactivation of catalysts Ag(0) NPs also confirmed that poisoning of catalysts was insignificant. This work promises sound environmental safety for several water-based systems against dye pollution.

3. Conclusion

In this study, nano-sized spherical Ag(0) NPs were synthesized with the help of erythromycin as a reducing agent as well as stabilizing agent. These nanoparticles were stable in solution for a very long time without any aggregation. The synthesized nanoparticles were confirmed by characterization techniques such as UV-Vis, SEM, HR-TEM, XRD, and FT-IR. The interaction of bonding formation was confirmed by FT-IR spectrophotometer. The morphology of Ag(0) NPs was observed by HR-TEM analysis and crystalline pattern was confirmed by powder XRD. The synthesized Ag NPs were confirmed as the best catalyst with enhanced rates of reduction for EB, MB, and RB. The present study is the first report about the use of erythromycin Ag(0) NPs as reduction catalysts for EB, MB, and RB and is expected to open new doors for their further catalytic applications in analogous and other experiments compassing environmental and industrial usage.

4. Experimental

4.1. Chemicals

All chemicals and reagents (NaOH, $AgNO_3$, $NaBH_4$, RB, MB, and EB) used in this study were of high purity and analytical grade. Erythromycin was purchased from Fluka.
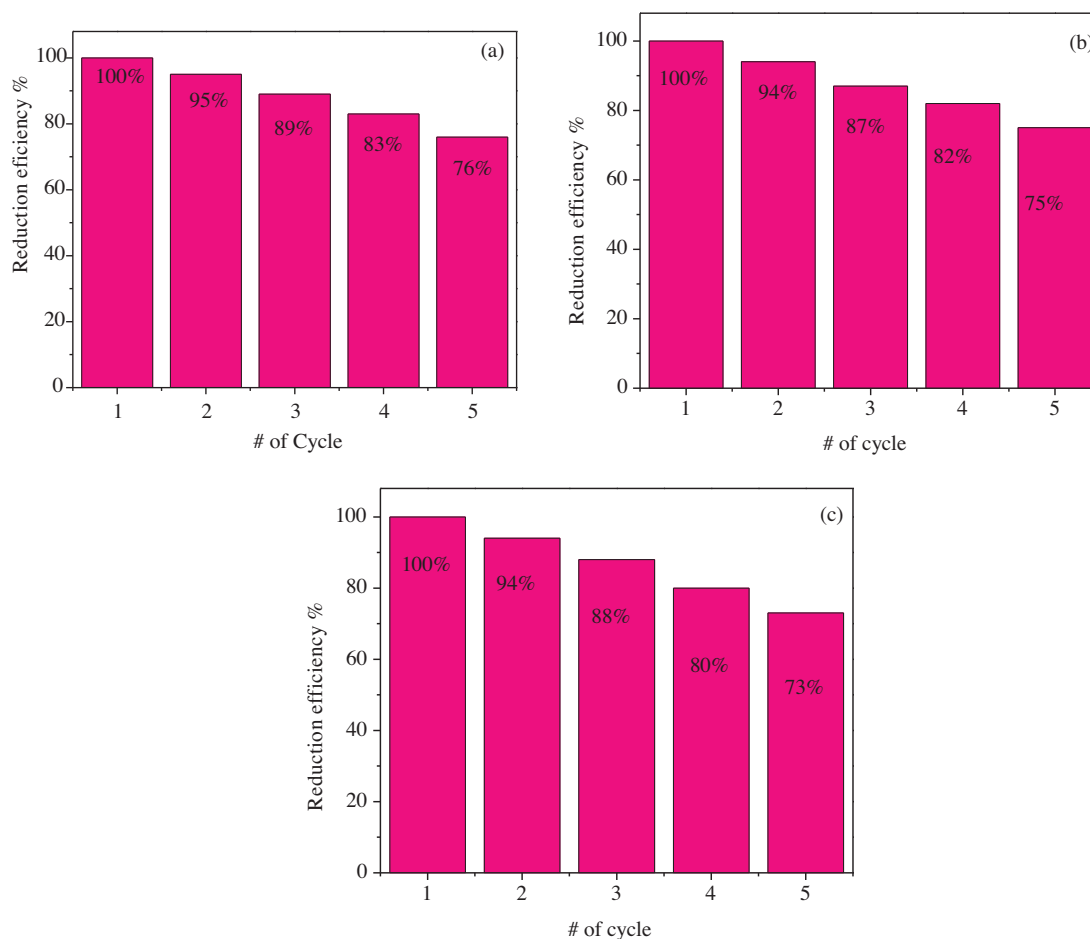
Figure 9. The efficiency of Ag(0) NPs for the reduction of dyes: (a) MB, (b) RB, (c) EB.

4.2. Instrumentation

UV-Vis spectra of Ag(0) NPs containing solution were recorded with a model Lambda 2 spectrometer from PerkinElmer.

An analytical scanning electron microscope (ASEM) model JSM 6380A from Jeol Company was used for SEM imaging of a dried drop from Ag(0) NPs containing solution on a microscopic glass cover slip just after coating with a gold layer for 5 min duration in a DC ion sputter model JFC-1500.

FT-IR spectra were recorded in transmission mode (PerkinElmer BX FT-IR) on powder samples that were ground with KBr and compressed into a pellet. FT-IR spectra in the range 4000–400 cm^{-1} were recorded in order to investigate the nature of the chemical bonds formed.

X-ray powder diffraction (XRD) analysis was conducted on a Rigaku Smart Lab Diffractometer operated at 40 kV and 35 mA using Cu Kα radiation.

High resolution transmission electron microscopy (HR-TEM) analysis was performed using a JEOL JEM 2100 microscope. A drop of diluted sample in alcohol was dripped on a TEM grid.

4.3. Synthesis of erythromycin-derived Ag(0) NPs

For a typical synthesis, 0.05 mL of erythromycin standard solution was mixed with 0.1 mL of $AgNO_3$ (0.5%) and 0.03 mL of NaOH solutions to synthesize Ag(0) NPs. The accelerating property of Ag(0) NPs was observed by measuring the UV-Vis spectra. Here we highlight the use of erythromycin as reducing as well as capping agent for fabrication of silver nanoparticles.

4.4. Catalysis study of silver nanoparticles

The catalytic effectiveness of silver nanoparticles was monitored for MB, RB, and EB. The catalytic reduction of these dyes was carried out in a standard quartz cell with 1-cm path length and about 3-mL volume containing Ag(0) NPs encumbered pieces of glass. Under optimized conditions, the catalytic reaction procedure for MB, RB, and EB was performed as follows: 0.4 mL (100 μM) of each dye was taken individually in a quartz cell followed by the addition of 2.80 mL of Milli Q water then adding 0.4 mL of 0.1 M $NaBH_4$. After careful and immediate addition of 0.15 mg of Ag(0) NPs, they were immobilized on pieces of glass and put in a quartz cell for the reduction process. The absorption spectra were monitored by a UV-Vis spectrophotometer with a time interval of 50 s in a scanning range of 400 to 700 nm.

Acknowledgments

References

1. Sondi, I.; Goia, D. V.; Matijevic, E. *J. Colloid Interface Sci.* **2003**, *260*, 75–81.

2. Edison, T. I.; Sethuraman, M. G. *Process. Biochem.* **2012**, *47*, 1351–1357.

3. Aksomaityte, G.; Poliakoff, M.; Lester, E. *Chem. Eng. Sci.* **2013**, *85*, 2–10.

4. Darroudi, M.; Zak, A. K.; Muhamad, M. R.; Huang, N. M.; Hakim, M. *Mater. Lett.* **2012**, *117*, 117–120.

5. Kim, S. E.; Park, J. H.; Lee, B.; Lee, J. C.; Kwon, Y. K. *Radiat. Phys. Chem.* **2012**, *81*, 978–981.

6. Balamurugan, A., Ho, K. C.; Chen, S. M. *Synth. Met.* **2009**, *159*, 2544–2549.

7. Tagar, Z. A.; Sirajuddin, Memon, N.; Agheem M. H.; Junejo, Y.; Hassan, S. S.; Kalwar, N. H.; Khattak, M. I. *Sens. Actuators B* **2011**, *157*, 430-37.

8. Junejo, Y.; Karaoğlu, E.; Baykal, A.; Sirajuddin *J. Inorg. Organomet. Polym.* **2013**, *23*, 970–975.

9. Kouvaris, P.; Delimitis, A.; Zaspalis, V.; Papadopoulos, D.; Tsipas, S. A.; Michailidis, N. *Mater. Lett.* **2012**, *76*, 18–20.

10. Jagtap, U. B.; Bapat, V. A. *Ind. Crops Prod.* **2013**, *46*, 132–137.

11. Bar, H.; Bhui, D. K.; Sahoo, G. P.; Sarkar, P.; Pyne, S.; Misra, A. *Colloids Surf. A: Physicochem. Eng. Aspects* **2009**, *348*, 212–216.

12. Saha, S.; Wang, J. M.; Pal, A. *Sep. Purif. Technol.* **2012**, *89*, 147–159.

13. Nanda, A.; Saravanan, M. *Nanomedicine: Nanotechnology Biology and Medicine* **2009**, *5*, 452–456.

14. Cho, K. H.; Park, J. E.; Osaka, T.; Park, S. G. *Electrochim. Acta* **2005**, *51*, 956–960.

15. Sondi, I.; Sondi, B. S. *J. Colloid Interface Sci.* **2004**, *275*, 177–182.

16. Shahverdi, A. R.; Fakhimi, A.; Shahverdi, H. R.; Minaian, S. *Nanomedicine: Nanotechnology Biology and Medicine* **2007**, *3*, 168–171.

17. Maneerung, T.; Tokur,a S.; Rujiravanit, R. *Carbohydr. Polym.* **2008**, *72*, 43–51.

18. Pradhan, N.; Pal, A.; Pal, T. *Langmuir* **2001**, *17*, 1800–1802.

19. Burda, C.; Chen, X.; Narayanan, R.; El-Sayed, M. A. *Chem. Rev.* **2005**, *105*, 1025–1102.

20. Siani, A.; Wigel, K. R.; Alexeev, O. S.; Amiridis, M. D. *J. Catal.* **2008**, *257*, 5–15.

21. Cortie, M. B.; Van der Lingen, E. *Mater. Forum* **2002**, *26*, 1–14.

22. Brown, M. A.; De Vito, S. C. *Crit. Rev. Environ. Sci. Technol.* **1993**, *23*, 249–324.

23. Safarik, I.; Ptackova, L.; Safarikova, M. *Eur. Cell Mater.* **2002**, *3*, 52–55.

24. Lin, J.; Zong, R.; Zhou, M.; Zhu, Y. *Appl. Catal. B: Environ.* **2009**, *89*, 425–431.

25. Ibhadon, A. O.; Greenway, G. M.; Yue, Y. *Catal. Commun.* **2008**, *9*, 153–157.

26. Lachheb, H.; Puzenat, E.; Houas, A.; Ksibi, M.; Elaloui, E.; Guillard, C.; Herrmann, J. M. *Appl. Catal. B: Environ.* **2002**, *39*, 75–90.

27. Ferreira-Leitao, V. S.; da Silva, J. G.; Bon, E. P. S. *Appl. Catal. B Environ.* **2003**, *42*, 213–221.

28. Daneshvar, N.; Aleboyeh, A.; Khataee, A. R. *Chemosphere* **2005**, *59*, 761–767.

29. Jana, N. R.; Wang, Z. L.; Pal, T. *Langmuir* **2000**, *16*, 2457–2463.

30. Fan, J.; Guo, Y.; Wang, J.; Fan, M. *J. Hazard. Mater.* **2009**, *166*, 904–910.

31. Sau, T. K.; Pal, A.; Pal, T. *J. Phys. Chem. B* **2001**, *105*, 9266–9272.

32. Martin, C. F.; Birot, M.; Deleuze, H.; Desforges, A.; Backov, R. *React. Funct. Polym.* **2007**, *67*, 1072–1082.

33. Kumar, P.; Govindaraju, M.; Senthamilselvi, S.; Premkumar, K. *Colloids Surf. B* **2013**, *103*, 658–661.

34. Kalwar, N. H.; Sirajuddin; Sherazi, S. H.; Khaskheli, A. R.; Hallam, K. R.; Scott, T. B.; Tagar, Z. A.; Hassan, S. S. Appl. Catal. A: Gen. 2013, 453, 54–59. 35. Peng, H.; Yang, A.; Xiong, J. *Carbohydr. Polym.* **2013**, *91*, 348–355.

35. Philip, D.; Unni, C.; Aromal, S. A.; Vidhu, V. K. *Spectrochim. Acta A* **2011**, *78*, 899–904.

36. Wejrzanowski, T.; Pielaszek, R.; Opalinska, A.; Matysiak, H.; Łojkowski, W.; Kurzydowski, K. J. *Appl. Surf. Sci.* **2006**, *31*, 253–264.